Earth Reinforcement, Ochiai, Yasufuku & Omine (eds) © 1996 Balkema, Rotterdam. ISBN 905410 833 9

Dynamic response analysis of geogrid reinforced steep embankment subjected to an earthquake

T. Fujii, N. Fukuda & N. Tajiri
Fukken Co., Ltd, Consulting Engineers, Hiroshima, Japan

ABSTRACT: A geogrid reinforced steep embankment 6.5 m high at a distance of 33 km from the epicenter was subjected to the Kushiro offshore earthquake of January 1993, but kept its stability. The maximum seismic acceleration was estimated at 310 gal. This embankment proved to have a high aseismatic performance, because although it had been designed under the ordinary condition only, it maintained its stability during the earthquake.

In the first place, seismic response analysis by the total stress method using actual seismic waves was performed. Then, evaluation of stability by the seismic coefficient method was reviewed by the current Japanese design method (PWRI). From these analyses, the following findings were obtained; 1)The reinforced zone behaved as an integrated soil mass, and 2) direct sliding did not occur since the horizontal earth pressure in the back of the reinforced zone did not reach the maximum level at the time of maximum inertia force of the reinforced zone.

1 INTRODUCTION

To date many design methods for geosynthetic reinforced soil walls and steep-sloped embankments have been presented. Seismic design methods among them are based on shaking table experiments and the seismic coefficient method. However, the seismic design methods have yet to be verified based on such soil structures subjected to actual earthquakes. Collin, et al. (1992) investigated some reinforced soil structures near the epicenter of the 1989 Roma Prieta earthquake (M7.1) and reported that those structures demonstrated high seismic performance. Fukuda, et al. (1994) performed a stability analysis using the seismic coefficient method on a reinforced steep embankment 6.5 m high which had been subjected to the 1993 Kushiro offshore earthquake (M_J7.8) and maintained its stability under the estimated horizontal acceleration of 310 gal. Besides, Tatsuoka, et al. (1995) reported that geosynthetic reinforced soil walls demonstrated their high seismic stabilities under the 1995 Hyogoken-nanbu earthquake (M_J7.2).

This paper describes a seismic response analysis conducted, following the above-mentioned static analysis of Fukuda, et al., by using actual wave forms recorded during the Kushiro offshore earthquake and presents the findings for the seismic stabilities of reinforced soil structures.

2 CONDITIONS OF REINFORCED STEEP-SLOPE EMBANKMENT

2.1 *Foundation and embankment*

As shown in Fig.1 the reinforced embankment is constructed on the foundation covered by topsoil of 1 m thickness. This foundation is underlain by the alluvium on rock, which consists of 1 m-thick gravelly soil layer with a SPT N-value of approximately 5 to 10.

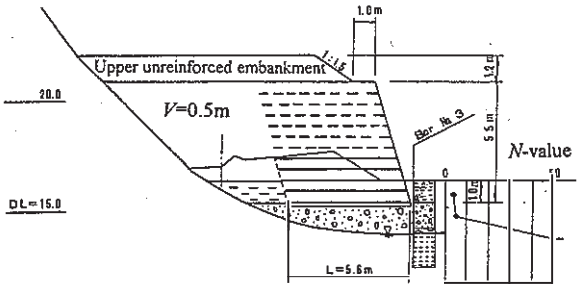

Fig. 1 Standard cross section of reinforced embankment.

On the foundation formed by stripping off 1 m-thick topsoil, the embankment was constructed to a height of 5.5 m with the face slope 73.3° and height of upper unreinforced embankment of 1.2 m. The front area of the embankment was backfilled (1 m-thickness) to the

Table 1 Soil properties of fill material.

Soil parameters		Properties
Specific gravity	G_S	2.65
Natural water content	w_n (%)	40.6
Liquid limit	w_L (%)	48.0
Plastic limit	w_p (%)	32.7
Plasticity index	I_p	15.3
Fine fraction	F (%)	49.0
Maximum dry unit weight	γ_{dmax} (kN/m³)	13.0
Optimum moisture content	w_{opt} (%)	34.4

previous surface level after the construction of embankment.

The filling material is of volcanic cohesive soil (SV). Table 1 shows the properties of the filling material. The designed shear strength parameters of the filling material are: internal friction angle $\phi'=25^{\circ}$, cohesion $c'=0$ kPa, and unit weight $\gamma=17.6$ kN/m^3, although the results obtained from the test are $\phi'=27.0^{\circ}$ and $c'=6.9$ kPa.

2.2 *Design*

In Japan the steep slope reinforced embankments had mostly been designed in accordance with the Jewell et al.'s method (1984) until the publication of Japanese design method for reinforced soil structures (Geogrid Research Board; 1990, PWRI; 1992). This embankment also designed by Jewell et al.'s method under only the ordinary condition. In the design calculation, geogrids 5.6 m long with a tensile strength (T_f) of 49.0 kN/m and an allowable tensile strength (T_A) of 29.4 kN/m were laid as reinforcement with vertical spacing (V) of 0.5 m. However, in the sections represented by broken lines in Fig.1, 1 m-wide geogrids were laid in a staggered pattern at 1 m horizontal intervals, since the strength of the reinforcements exceeded the required tension.

The slope face of the geogrid reinforced embankment was protected by applying expanded metal units 0.5 m in height and 2.0 m in width as shown in Fig. 2.

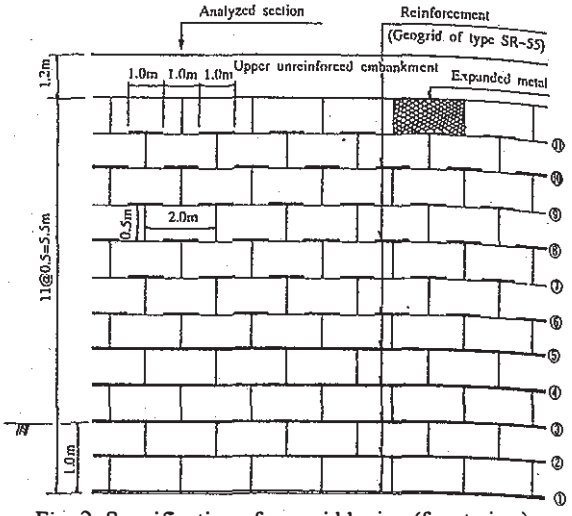

Fig. 2 Specification of geogrid laying (front view).

3 DYNAMIC RESPONSE ANALYSIS

3.1 *Analytical model and conditions*

In this study, two-dimensional dynamic response

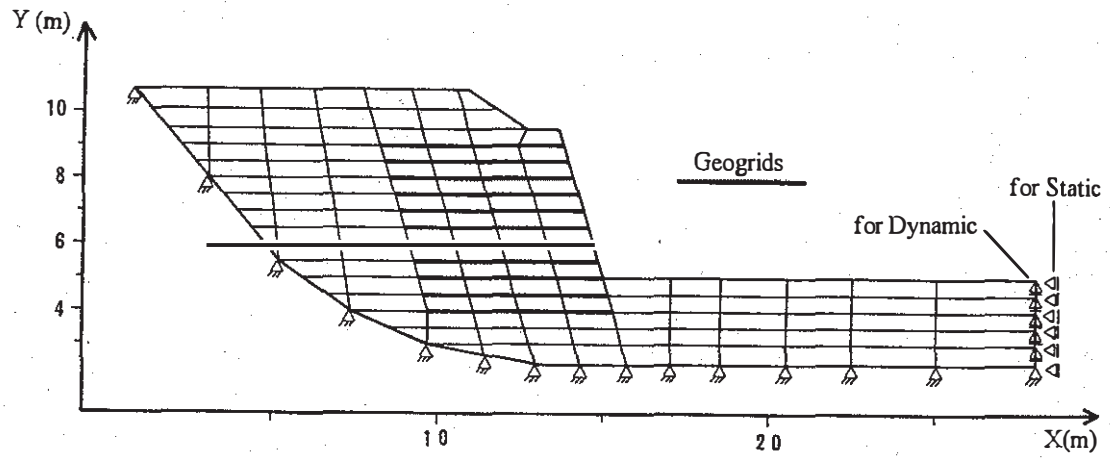

Fig. 3 Model of seismic response analysis.

Table 2 Soil parameters used in seismic response analysis.

Soil parameters		Banking soil	Sandy silt layer	Gravel layer
Wet unit weight	γ_t (kN/m^3)	17.6	17.6	20.6
Cohesion	c' (kPa)	6.9	15.0	0.0
Internal friction angle	ϕ' (degree)	27.0	0.0	34.5
Poisson's ratio ν	Static	0.3333	0.3333	0.3333
	Dynamic	0.4999	0.4999	0.4999
Shear modulus Coefficient to determine $G_0=\alpha \cdot \sigma_m^n$	α ((MPa)$^{1-n}$)	28.5	17.6	19.3
	n	0.4	0.4	0.4

Table 3 Material properties of geogrids used in seismic response analysis.

Material properties	1st-5th layers from bottom	6th-11th layers from bottom	Remarks
Elongation rigidity $E \cdot A$ (kN)	981	491	From result of tensile test
E ; Elastic modulus (kPa)	981	981	Temporary setting for input
A ; Sectional area (m^2)	1.0	0.5	
Moment of inertia of area I_z (m^4)	10^{-4}	10^{-4}	Estimated as tension member
Unit weight of geogrid γ_t (kN/m^3)	10^{-4}	10^{-4}	Value small enough Weight of giogrids disregarded

analysis was carried out using nonlinear dynamic FEM program SADAP which was developed by the Public Works Research Institute of the Ministry of Construction (PWRI, 1985). In this program, to explain the nonlinear stress-strain relationship of soil, the Hardin-Drnevich model was used on both static and dynamic analysis. And the step-by-step integration method was applied in time dimension to conduct the responce analysis.

Fig. 3 illustrates the analytical model of the reinforced embankment. Table 2 shows the soil parameters of each layer used in the analysis. The strength parameter of the banking soil was obtained from the result of an triaxial compression test, and those of the foundation from the N-values. The initial shear moduli (G_0) were calculated from N-values by the following equation:

$$G_0 = \rho \cdot V_S^2 \qquad (1)$$

where, V_S is the elastic wave velocity ($80N^{1/3}$ in case of sand layer and $100N^{1/3}$ in case of clay layer).

In the modelling of the embankment, the geogrid was treated as a beam element, and a joint element was provided between the geogrid and the banking soil due to the large difference between their rigidities. The material properties of the geogrid were set as indicated in Table 3.

3.2 *Setting of seismic motion*

Used in the analysis was the wave form (Fig. 4) in the east-west direction recorded on the alternating layers of sandstone and conglomerate in Akkeshi. The

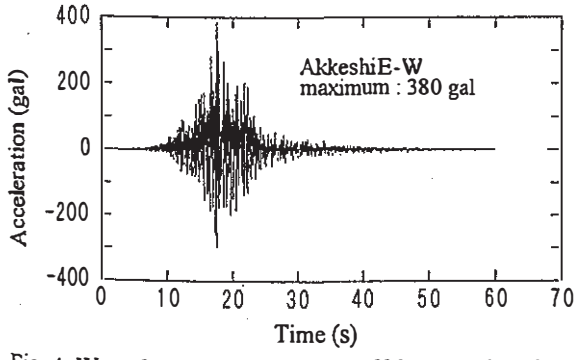

Fig. 4 Wave form of 1993 Kushiro offshore earthquake.

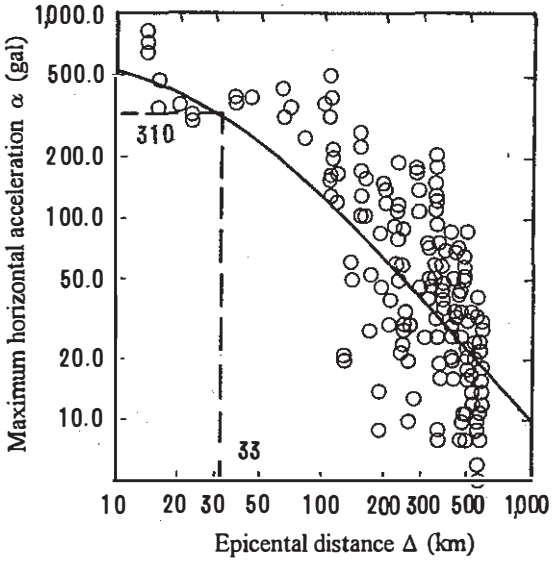

Fig. 5 Attenuation characteristic curve of peak ground acceleration (On the ground in $\Delta \leqq 600$ km, 116 sites).

characteristic of this wave form is that short-period elements of the order of 0.15 - 0.35 seconds were predominant and the duration of the main ground shaking was as relatively short as 25 - 30 seconds.

There have been proposed many equations which generally represent the maximum ground acceleration in the relation between the magnitude and the distance from the epicenter. In this study, it was determined from a attenuation characteristic curve for horizontal ground acceleration (Fig. 5) which was presented by the Coordinating Committee for Promotion of the Strong Motion Earthquake Observation Project (1993). The distance between the reinforced embankment and the epicenter (Δ) was 33 km and the maximum horizontal acceleration (α_{max}) was estimated at 310 gal.

In this analysis, the accelerations was input as only horizontal shaking from the base of N-value over 50.

3.3 *Response acceleration and deformation*

Fig. 6 (a) shows the distribution of the horizontal maximum response acceleration, where the horizontal acceleration increases toward the top of the slope face and to as large as 350 gal.

Fig. 6 (b) shows the distribution of the vertical

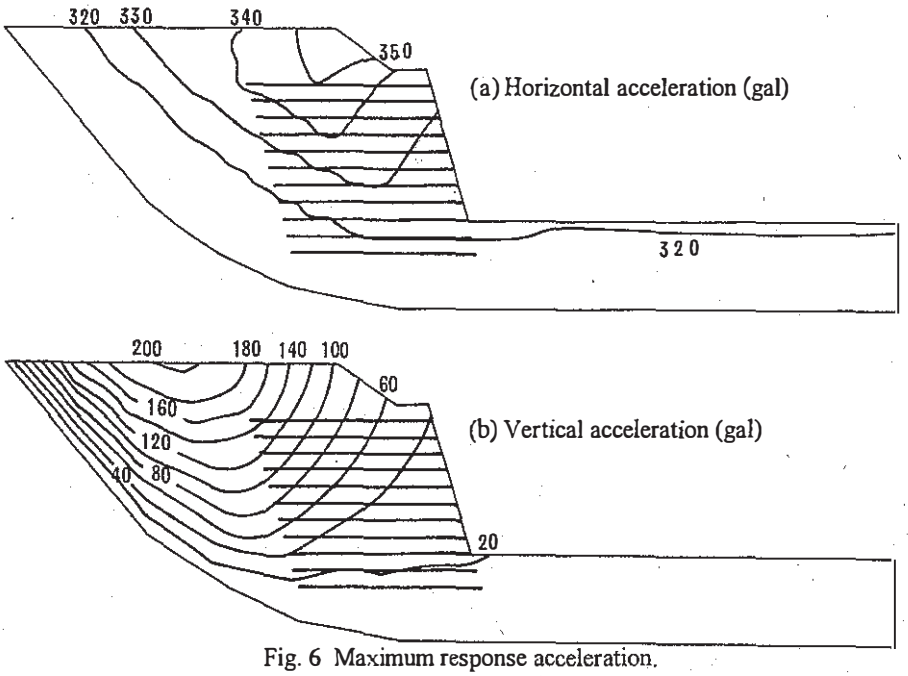

Fig. 6 Maximum response acceleration.

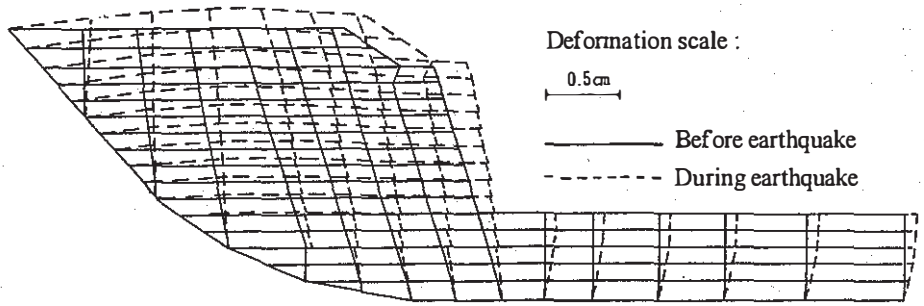

Fig. 7 Maximum Deformation.

maximum acceleration, where the vertical acceleration increases toward the top of the embankment and, in particular an acceleration as large as 200 gal developed in the non-reinforced back area of the embankment. The times of occurrence of the horizontal and vertical maximum accelerations almost coincided with each other.

Fig. 7 shows the maximum deformation of the embankment during the earthquake. It can be observed that in the condition where the maximum deformation occurred on the slope face, the embankment presented upward displacement, which corresponded with the tendency of the response acceleration.

3.4 *Principal stress and tension of geogrids*

Fig. 8 shows the distribution of the principal stress during the earthquake. It can be observed from this figure that the directions of the principal stresses of the elements in the geogrid-reinforced zone are not slant, indicating the development of little shearing stresses.

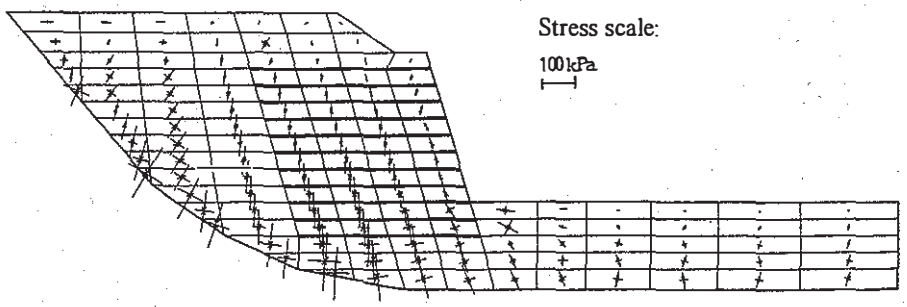

Fig. 8 Distribution of principal stress.

On the other hand, in the zones in front and at the back of the reinforced zone, the principal stresses show heavy slants, indicating the development of large shearing stresses. These results are suggestive that the geogrid-reinforced soil mass took an integrated behavior during the earthquake.

Focusing on the elements at the back of the reinforced zone, we compared the horizontal stress before the earthquake and that at the time of development of the maximum horizontal acceleration in the reinforced zone. The result is shown in Fig. 9, from which it can be observed that the back zone's earth pressure was reduced in the condition that the maximum horizontal inertia force acted on the reinforced zone. This finding differs from the conventional conception in the seismic design that the horizontal inertia force in the reinforced zone and the seismic earth pressure in the back zone act simultaneously.

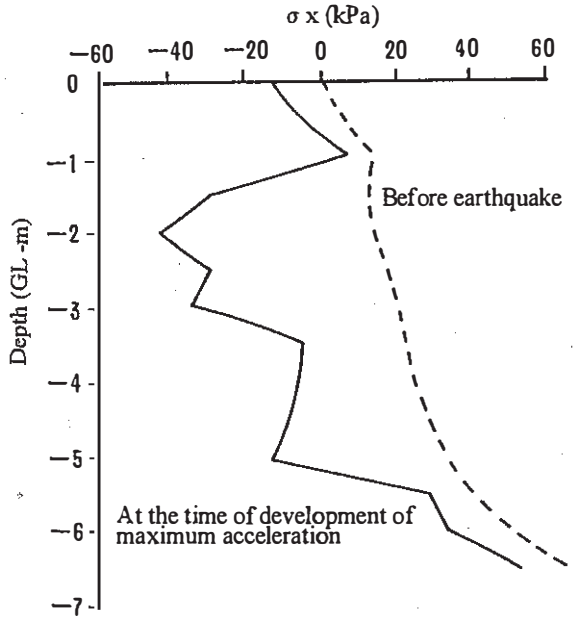

Fig. 9 Variation of horizontal stress in the back area.

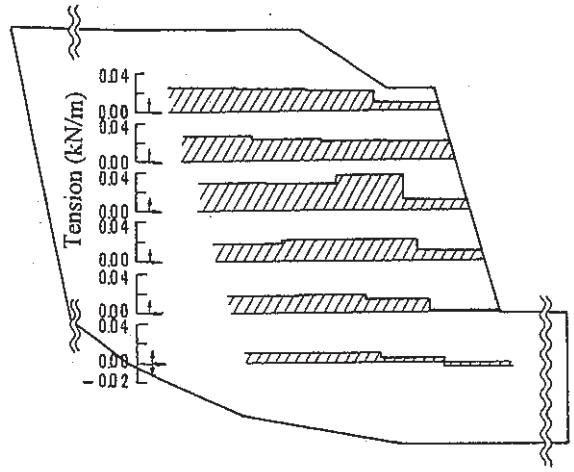

Fig. 10 Distribution of tension on geogrids.

Fig. 10 shows the distribution of the maximum tensions of geogrids during the earthquake. As shown in this figure, tensions developed in almost whole area of the embankment, but they were small, even the maximum of which was only 0.4 kN/m. They are minuscule when compared with the geogrid's tensile strength, T_f, of 49 kN/m suggesting that development of large stresses in a reinforced soil mass can be avoided if the reinforced mass takes an integrated behavior.

4 DISCUSSION OF SEISMIC STABILITY

Table 4 shows the result of the stability analysis of the embankment under the average responce acceleration of 330 gal from Fig. 6 (a). The design method of the PWRI was used in this analysis. The safety factor of the circular slip through the reinforced zone turned out to be 1.03, indicating that the embankment maintained the stability almost in its critical condition. It can be assumed that the tensions on the upper reinforcements exceeded their tensile strength. On the otherhand, the safety factor against direct sliding of reinforced zone as pseudo-retaining wall becomes critical state of 1.01.

However, based on the results of the response analysis, smaller earth pressure as ordinary condition instead of the simultaneous seismic earth pressure in the back zone, the safety factor against direct sliding turns out to be a sufficient value as 1.23.

$$F_{Sd}=\frac{\tan\phi'(W_1+P_V)}{k_h W_1+P_H}=\frac{0.51\times(527-10)}{0.34\times527+35}=1.23 \qquad (2)$$

These are the reason of the fact that the embankment maintained its stability that prove to have high aseismatic performance of reinforced soil structure.

Table 4 Results of stability analysis by PWRI method.

Design condition			Test parameters
γ_t (kN/m³)			17.6
c' (kPa)			6.9
ϕ' (degree)			27.0
k_h			0.34
T_f (kN/m)			49.0
T_A (kN/m)			29.4
T_{AE} (kN/m)			44.1(=1.5T_A)
	F_S of slip circle		F_S = 1.03> 1.0
Internal stability	Tension at reinforcement	Layer No.*	Tension T_i (kN/m)
		⑩	49.0 << 69.3
		⑥	29.4 < 49.0 < 44.1
		⑥	29.4 < 38.8 < 44.1
		⑤	13.3 < 29.4
		④	13.6 < 29.4
		③	7.0 < 29.4
External stability	F_{Sd} of direct sliding		F_{Sd} = 1.01 < 1.2
	Overturning (m)		e = 0.21 < L/3 = 1.87
	Bearing capacity (kPa)		q_{max} = 118.7 < 294.0

Notes : The figure in ( ) is acording to GRB method. * : Refer to Fig. 2.

5 CONCLUSIONS

Dynamic responce analysis and static analysis using the seismic coefficient method are applied for a reinforced steep-slope embankment subjected to the 1995 Kushiro offshore earthquake. The following are the findings:

(1) Although only horizontal seismic acceleration was inputted, vertical seismic shaking developed in the embankment. In the condition that the vertical displacement in the embankment occurred upward, the horizontal displacement of the slope face became maximum.

(2) The embankment took an integrated behavior under the seismic shaking, and there developed no so large tensile forces in the reinforcements as static design methods indicate.

(3) When the maximum horizontal acceleration developed in the reinforced area, observed in the back area were horizontal stresses smaller than ordinary ones. There was observed a phase difference between the horizontal inertia force in the reinforced area and the seismic earth pressure in the back area, thus denying their simultaneous development which is assumed in the current design.

(4) Using simultaneously the maximum horizontal inertia force in the reinforced area and the ordinary earth pressure in the back area, we calculated the stability against sliding to find the factor of safety to be 1.23. This would be the reason why the embankment could maintain its stability during the earthquake.

It is necessary to make further, detailed study of the results of dynamic response analyses and reflect the study results in the conception of the seismic design.

ACKNOWLEDGEMENTS

The authors would like to express their heart-felt thanks to Mr. Osamu Matsuo and Mr. Takao Shimazu of the Public Works Research Institute of the Ministry of Construction for their technical guidance and valuable comments on this dynamic response analysis.

REFERENCES

Collin, J. G., V.E. Chouery-Curtis and R.R. Berg (1992). Field observation of reinforced soil structures under seismic loading, *Proc. Int. Symp. on Earth Reinforcement Practice (IS Kyushu '92)*, Fukuoka, Japan, Vol. 1, pp.223-228.

Coordinating Committee for Promotion of the Strong Motion Earthquake Observation Project (1993). *Strong motion earthquake quick report No. 41 the Kushiro offshore earthquake (1993)*. (in Japanese)

Fukuda, N., N. Tajiri, T. Yamanouchi, N. Sakai and H. Shintani (1994). Applicability of seismic design methods to geogrid reinforced embankment. *5th Int. Conf. on Geotextilles, Geomembranes and Related Products*, Singapore, Vol. 1, pp.533-536.

Geogrid Research Board (1990). *Geogrid construction method guideline*, Vols. 1 and 2, 244p and 150p. (in Japanese)

Jewell, R. A., N. Paine and R. I. Woods (1984). Design method for steep reinforced embankments, *Symp. of Polymer Grid Reinforcement in Civil Eng.*, London, pp.70-81.

Public Works Research Institute, Ministry of Construction (1985). SADAP User's Manual. (in Japanese)

Public Works Research Institute, Ministry of Construction (1992). *Design and construction manual of geotextile-reinforced embankments, Technical memorandum of Public Works Research Institute*, No. 3117, 404p. (in Japanese)

Tatsuoka, F., J. Koseki and M. Tateyama (1995). Performance of geogrid-reinforced soil retaining walls during the Great Hanshin-Awaji Earthquake, January 17, 1995, *Ist Int. Conf. on Earthquake Geotechnical Engineering (IS-Tokyo '95)*, Tokyo, Japan, Vol. 1, pp.55-62.